Size Matters More Than Chemistry for Cloud-Nucleating Ability of Aerosol Particles

U. Dusek,[1] G. P. Frank,[1] L. Hildebrandt,[1,4] J. Curtius,[3] J. Schneider,[2] S. Walter,[2] D. Chand,[1] F. Drewnick,[2] S. Hings,[2] D. Jung,[3] S. Borrmann,[2,3] M. O. Andreae[1]

Size-resolved cloud condensation nuclei (CCN) spectra measured for various aerosol types at a non-urban site in Germany showed that CCN concentrations are mainly determined by the aerosol number size distribution. Distinct variations of CCN activation with particle chemical composition were observed but played a secondary role. When the temporal variation of chemical effects on CCN activation is neglected, variation in the size distribution alone explains 84 to 96% of the variation in CCN concentrations. Understanding that particles' ability to act as CCN is largely controlled by aerosol size rather than composition greatly facilitates the treatment of aerosol effects on cloud physics in regional and global models.

The response of cloud characteristics and precipitation processes to increasing anthropogenic aerosol concentrations is one of the largest uncertainties in the current understanding of climate change (1, 2). A major challenge is to determine the ability of aerosols to act as cloud condensation nuclei (CCN) at water vapor supersaturations S (percentage of relative humidity minus 100%) that are relevant for atmospheric conditions. CCN activation of aerosols is therefore being studied intensively in laboratory and field experiments (3–10). To a first approximation, the ability of a particle to act as a CCN at a given S depends on the number of potential solute molecules it contains, which is a function of its size and composition. Thus, knowledge of both particle size distribution and size-resolved particle composition is necessary to predict ambient CCN concentrations (11). Although size distributions can be measured automatically in situ or even remotely, the determination of aerosol chemical composition is much more demanding. Moreover, the effects of organic compounds on CCN activation are not completely understood (12). If the effects of chemical composition on CCN activation could be parameterized for certain regions or aerosol types, this would considerably simplify estimation and modeling of CCN concentrations. It is therefore of great importance to assess the relative contributions of particle size distribution and chemical composition to CCN activity.

Toward this goal, we investigated the CCN activation of aerosols as a function of preselected particle sizes, to separate the effect of particle composition from that of size. This technique is commonly used in the laboratory (3–6) but rarely in the ambient atmosphere (13, 14). We used a differential mobility analyzer to select a narrow particle size range from the total aerosol population. These particles were passed to a CCN counter (15), which measured the number of activated CCN as a function of S, while a condensation particle counter in parallel determined the total particle concentration (CN) in the selected size fraction. This information was used to derive the CCN/CN ratio at each particle diameter and S. The size-resolved CCN/CN ratio is further referred to as CCN efficiency (16).

The S at which particles of equal size are activated is dependent on particle composition and/or shape. For monodisperse particles, the dependence of the CCN efficiency on S (the CCN spectrum) can therefore serve as an empirical measure of all chemical effects on CCN activation, including the effects of slightly soluble organics (17) and of surface active compounds (18). Additionally, possible external mixtures of particles with respect to their CCN properties can be identified (19).

Size-resolved CCN measurements were conducted during the Feldberg Aerosol Characterization Experiment (FACE-2004) field experiment, which took place at the Taunus Observatory (50.2°N, 8.4°E; Kleiner Feldberg, central Germany) from 20 July until 11 August 2004. During the measurement period, diverse air masses were encountered, including aged continental air masses, marine air masses that had moved in rapidly from the North Atlantic, and fresh pollution from the densely populated and industrialized Rhine-Main area, ~20 km to the southeast and southwest of the field site.

Figure 1A shows a representative example of 6-hour averaged CCN efficiencies. At S between 0.25 and 1.5%, the crucial size range for CCN activation is 40 to 120 nm (electrical mobility diameter, d_p). Particles much larger than $d_p = 120$ nm are generally activated at all investigated values of S regardless of their composition, whereas particles <40 nm require unrealistically high S for activation. Between these two extremes, a strong dependence of CCN efficiency on particle size is apparent. Particles with diameters of 40 nm typically require S of up to 1.5% for activation, whereas particles with diameters of 80 nm require S of ~0.5%. The question to be addressed here is whether the effect of particle composition on CCN activation can rival its strong dependence on size.

We illustrate this problem by comparing measurements in air masses representing extremes of chemical compositions encountered
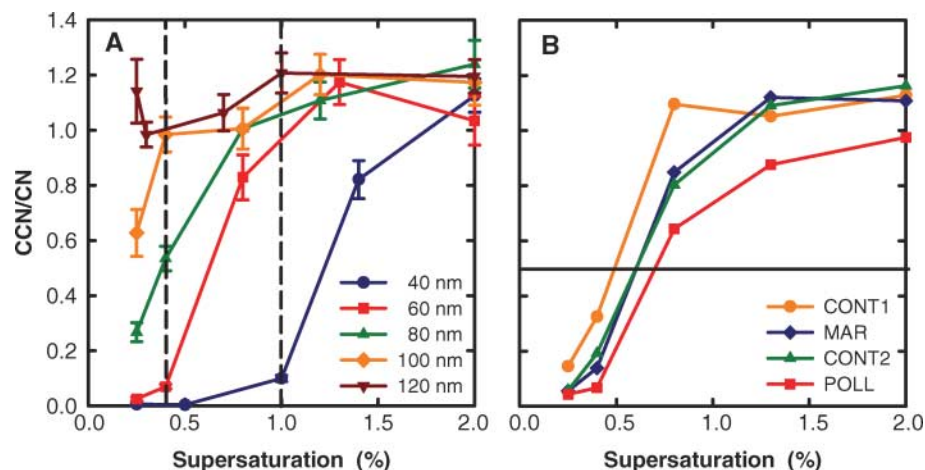

Fig. 1. (A) An example of size-resolved 6-hour averaged CCN spectra for particle diameters between 40 and 120 nm. Sixteen individual spectra have been averaged for each diameter. Error bars correspond to 95% confidence intervals of the mean. Vertical lines indicate the S values of 0.4 and 1% for which CCN size distributions are derived. CCN/CN ratios that are higher than 1 are due to a small bias in the calibration of the sensing volume, which probably changed slightly during the transport of the instrument to the field site. **(B)** The CCN spectra of particles with $d_p = 60$ nm are compared for different air mass conditions: CONT1 represents aged industrial pollution, MAR aerosol with Atlantic origin and short transport times over land, CONT2 rural continental aerosol, and POLL urban aerosol after a few hours of aging.

[1]Department of Biogeochemistry, [2]Department of Particle Chemistry, Max Planck Institute for Chemistry, Mainz 55128, Germany. [3]Johannes Gutenberg University, Institute for Atmospheric Physics, Mainz 55128, Germany. [4]California Institute of Technology, Pasadena, CA 91125, USA.

Table 1. Overview of the four air mass cases selected for the case study. The particle chemical composition refers to the size range from $d_p = 0$ to 130 nm, averaged over the respective measurement periods. "Inorg." stands for the mass concentration of NH_4^+, SO_4^{2-}, and NO_3^-; "Org." for the mass concentration of organic material; and "Inorg./total" for the mass fraction of inorganic material. The influence of recent pollution from the Frankfurt region was identified by local wind directions from the southeast. The origin of the air mass was determined by 4-day air mass back trajectories [see supporting online material C (16)].

	Time period	Inorg. (µg/m³)	Org. (µg/m³)	Inorg./total	Recent pollution	$S = 0.4\%$ cutoff diameter (nm)	Air mass origin
CONT1	7/31 18:00 − 8/1 18:00	1.72	2.38	0.42	No	66	Industrial (Ruhr region)
MAR	7/27 00:00 − 7/28 00:00	0.42	0.86	0.33	No	72.5	Atlantic
CONT2	7/22 00:00 − 7/23 00:00	0.66	1.92	0.26	No	73.6	France
POLL	8/2 12:00 − 8/3 18:00	0.47	2.13	0.18	Yes	83.4	N. Germany and Denmark

during FACE-2004 (Table 1 and Fig. 1B) (16). Two continental cases are considered: CONT1 is characterized by air masses arriving from heavily industrialized regions in the Netherlands and Germany, and CONT2 by air masses from more rural areas in France and southern Belgium. MAR represents marine air masses from the Atlantic, with transport times across Germany of less than 1 day. Local trajectories and wind directions (northwest to east) indicate that in these three cases, the air reached our site after traveling over forested areas for a few hours. Case POLL gives an example of recent pollution during southeasterly wind conditions (from the Frankfurt/Rhine Main area). For back trajectories, see fig. S3.

The composition of the nonrefractory aerosol components was measured by an Aerosol Mass Spectrometer (AMS) (20) in the size range from 40 to 1000 nm (16). In the CCN-relevant size range of $d_p < 130$ nm, the composition was dominated by organic material, followed by ammonium, sulfate, and nitrate. During CONT1, the mass fraction of inorganic ions in this size range was as high as 42%, whereas case POLL contained very little inorganic material, only 18% by mass for particles with $d_p < 130$ nm. The aerosol chemical compositions observed during the campaign span the range that is typical of near-urban to background sites in Europe (21). In the size range of $d_p < 150$ nm, soluble ions rarely make up more than 50% by mass (11, 21). On the other hand, soluble-ion fractions <15% are mostly found close to sources and in urban areas and increase quickly during atmospheric aging and mixing processes. Typically, about 50% of the organic fraction is also water-soluble and contributes to CCN activity (22).

Figure 1B shows that, in spite of the diverse origins and compositions of the aerosols in these four air mass types, the CCN spectra for a fixed size class (here 60 nm) resemble each other very closely. The S at which 50% of the particles are activated varies by only ± 0.1% around the mean value of 0.6% for this size class.

To derive the size distributions of CCN at a given S (for example, at 0.4 and 1%, Fig. 2), the size-resolved CCN spectra (Fig. 1A) are combined with aerosol number size distributions. First, the CCN efficiencies are linearly interpolated to $S = 0.4$ and 1% (dashed lines, Fig. 1A).
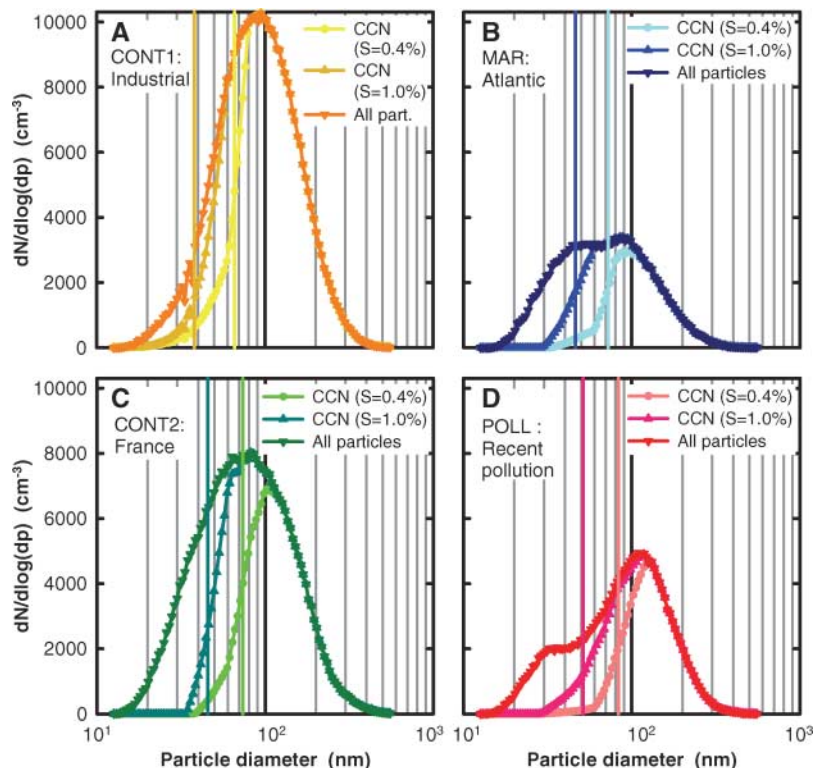
Fig. 2. (A to D) Particle number size distributions and CCN size distributions for the four chosen case studies. The colored vertical lines indicate the respective cutoff diameters: (the diameters where 50% of the particles are activated) at $S = 0.4\%$ and $S = 1.0\%$.

The resulting dependence of CCN efficiency on particle size is then used to derive the CCN size distributions (Fig. 2). For each value of S, the CCN concentration gradually increases toward larger diameters (Fig. 2), instead of showing a sharp cutoff activation diameter, as expected from an internally mixed aerosol. This reflects a certain degree of external mixing in ambient aerosols, as well as the fact that the particles are not exactly monodisperse (23).

We define effective cutoff diameters for each S (indicated as colored vertical lines in Fig. 2) as that diameter where the CCN efficiency reaches 0.5. These effective cutoff diameters are inversely related to the inorganic ion fraction of particles with $d_p < 130$ nm (see Table 1 for $S = 0.4\%$), as would be expected because organic compounds are usually less CCN-active than inorganic salts

(6). However, an increase in inorganic ion content by more than a factor of 2 [reflecting the entire range of composition from fresh pollution (POLL) to aged aerosol (CONT1)] is associated with a decrease in the cutoff diameter of less than 20 nm.

Total CCN concentrations (CCN_{tot}) at a certain S, obtained by integration of the CCN size distributions in Fig. 2, depend both on the total particle concentration and on the fraction of particles activated at the given S, which is a function of both the shape of the size distribution and of particle composition. For example, in CONT1, high CCN efficiency combined with a large modal diameter leads to the highest CCN_{tot} observed during the campaign (~4500 cm⁻³ at $S = 0.4\%$). This is considerably higher than in CONT2 (~3000 cm⁻³), where both modal diameter and CCN efficiency are lower, whereas total particle concentrations are com-

parable [6300 cm^{-3} (CONT1) versus 5800 cm^{-3} (CONT2)].

We performed sensitivity studies to gain further insight into the roles of total number concentration, shape of the size distribution, and size-resolved CCN efficiencies (that is, particle chemical composition) in determining CCN$_{tot}$. As a base case, we calculated a time series of 6-hour averaged CCN$_{tot}$ for the entire measurement period, using the measured size distributions and CCN efficiencies. Then we calculated two modified CCN time series: (i) using fixed CCN efficiencies (campaign average) but variable size distributions, and (ii) using a fixed size distribution (campaign average) but variable CCN efficiencies reflecting variable chemical composition (16). A correlation of these modified time series with the base case shows that the size distribution has by far the dominant role in determining CCN$_{tot}$ (Fig. 3, A and B, for $S = 0.4\%$; fig. S4 for $S = 0.25$ and 1.0%). At constant composition and CCN efficiency (case i), variations in the size distribution alone explain from 84% (at $S = 0.25\%$) to 96% (at $S = 1\%$) of the temporal variation in CCN$_{tot}$. When, on the other hand, a constant mean size distribution (case ii) is assumed, detailed knowledge of the CCN efficiencies is not very helpful in predicting CCN$_{tot}$ ($R^2 \sim 0.3$).

To eliminate the effect of variable total particle concentrations, we investigated how the fraction of particles that can act as CCN (hereafter referred to as the activated fraction) depends on size distribution and CCN efficiencies. For this purpose, we conducted a similar sensitivity study for the activated fraction, calculated as CCN$_{tot}$/CN10, where CN10 denotes the total number concentration of particles >10 nm (Fig. 3, C and D, for $S = 0.4\%$; fig. S5 for $S = 0.25$ and $S = 1\%$). The main conclusion remains similar: Variations in the shape of the size distribution explain ~80% of the variation in the activated fraction at S ranging from 0.25 to 1%, whereas variations in the composition (CCN efficiency) explain only 20% ($S = 1\%$) to 63% ($S = 0.25\%$). Figure 3D clearly shows the weak effect that variations in chemical composition have when the size distribution is held constant. The low sensitivity of the activated fraction to CCN efficiency at high S is due to the fact that the activation happens at smaller particle size (Fig. 2), where the size distribution was particularly variable in our measurements. Only at a low S of 0.25% do the CCN efficiencies show some significant correlation with CCN$_{tot}$/CN10. Here, cutoff diameters are near the size mode, which makes the activated fraction relatively sensitive to small changes in composition. However, assuming constant mean CCN efficiencies still gives an adequate prediction of the activated fraction (fig. S5, A and B).

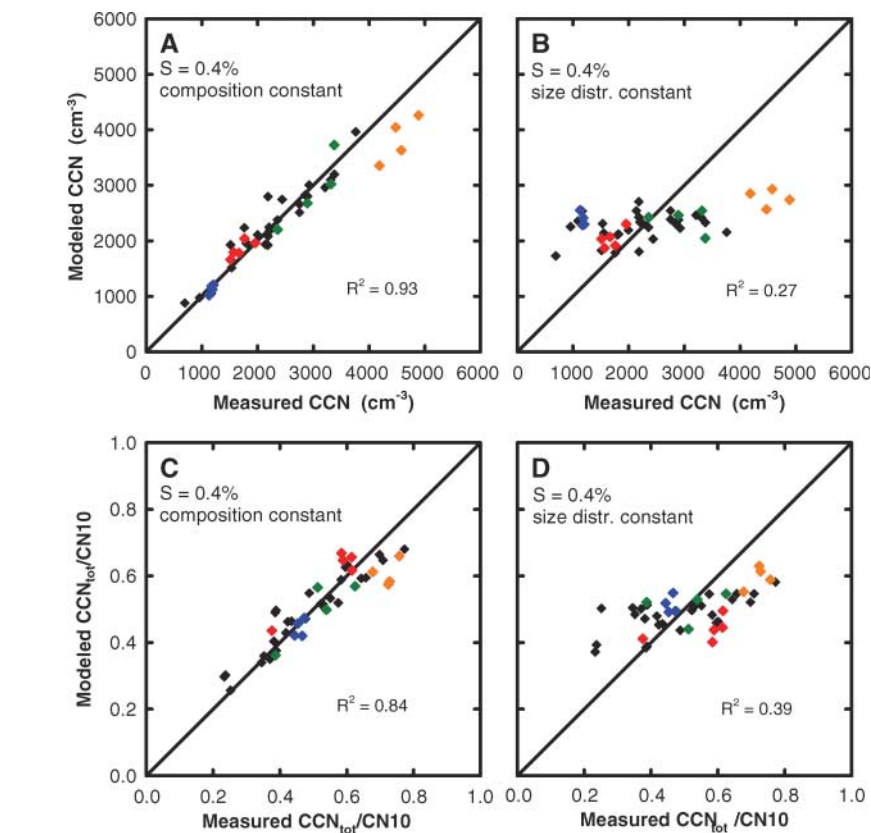These sensitivity studies confirm that it is more important to know the aerosol number

Fig. 3. (**A**) Correlation of the actual CCN concentration time series with a calculated time series derived using constant mean CCN efficiencies reflecting constant composition. Data points representing high CCN efficiencies tend to lie below the 1:1 line; data points representing low CCN efficiencies tend to lie above the 1:1 line. (**B**) Correlation of the actual CCN concentration time series with a calculated time series derived using constant mean size distributions but variable composition (CCN efficiencies). (**C**) same as (A) for activated fractions CCN$_{tot}$/CN10, (**D**) same as (B) for activated fractions CCN$_{tot}$/CN10. The data points corresponding to the case studies presented in Table 1 and Fig. 2 are marked in the respective colors.

size distribution accurately to achieve a good estimate of CCN$_{tot}$ than to know the detailed particle chemistry or precise size-resolved CCN efficiencies. This result is supported by model studies that suggest that the influence of particle composition on cloud droplet number is moderate (24), even if the effects of realistic mixtures of organic species are considered (25, 26). Our results show that in order to improve our understanding of atmospheric CCN, investigations of CCN activities of specific aerosol components must be complemented by careful studies of the aerosol size distribution and its dependence on atmospheric processes (27).

Although our results are from a continental site in Europe, we expect the primary role of particle size in CCN activation to apply generally. The fundamental reason is that the critical supersaturation (S_c) depends to first approximation on the total number of soluble molecules in the particle. This number depends only linearly on the soluble mass fraction, but to the third power on d_p, making particle size the dominant parameter in controlling S_c. Only in the case of insoluble particles, such as mineral

dust, can adding a trace amount of soluble material reduce S_c drastically (28, 29) and composition can then become dominant. The specific cutoff diameters can vary with aerosol type (for example, there are smaller cutoff diameters for marine aerosol). However, cutoff diameters derived for moderately aged biomass smoke and Amazonian background aerosols are nearly identical to those in our POLL case (30), making our results more generally applicable.

The secondary role of particle composition has great advantages for estimating CCN concentrations from observations and for their parameterization in cloud and climate modeling. With the knowledge of typical size-resolved CCN efficiencies (or cutoff diameters) that are representative of key regions and aerosol types, CCN concentrations can be estimated from observed or modeled size distributions. Establishing a database of such size-resolved CCN efficiencies should be the focus of field studies in different locations. For the purpose of modeling CCN on a global or local scale, more effort should be spent on

accurately predicting particle size distributions than on predicting detailed chemical composition. Although particle chemistry is important to model aerosol growth and transformation processes, the complex effects of particle chemical composition on CCN activation could be parameterized by cutoff diameters depending on location and/or aerosol type without introducing large errors. Assuming a "typical" size distribution (such as for a generalized "continental" aerosol) will lead to much larger errors than assuming a "typical" composition. Our findings also provide a basis for the estimation of CCN abundances over larger time and space scales by remote sensing, because aerosol size distributions are inherently more accessible by remote sensing than particle compositions. Because current sensors are limited, however, in their ability to detect particles in the CCN-relevant size range of 50 to 150 nm, this requires the development of appropriate sensors.

References and Notes

1. U. Lohmann, J. Feichter, *Atmos. Chem. Phys.* **5**, 715 (2005).
2. M. O. Andreae, C. D. Jones, P. M. Cox, *Nature* **435**, 1187 (2005).
3. H. Giebl *et al.*, *J. Aerosol Sci.* **33**, 1623 (2002).
4. K. Broekhuizen, P. P. Kumar, J. P. D. Abbatt, *Geophys. Res. Lett.* **31**, L01107 (2004).
5. M. Bilde, B. Svenningson, *Tellus* **56B**, 128 (2004).
6. T. M. Raymond, S. P. Pandis, *J. Geophys. Res.* **108**, 4787 (2002).
7. P. Y. Chuang *et al.*, *Tellus* **52B**, 843 (2000).
8. T. M. VanReken *et al.*, *J. Geophys. Res.* **108**, 4633 (2003).
9. G. C. Roberts, M. O. Andreae, J. Zhou, P. Artaxo, *Geophys. Res. Lett.* **28**, 2807 (2001).
10. J. R. Snider, J.-L. Brenguier, *Tellus* **52B**, 828 (2000).
11. G. McFiggans *et al.*, *Atmos. Chem. Phys. Discuss.* **5**, 8507 (2005).
12. R. J. Charlson *et al.*, *Science* **292**, 2025 (2001).
13. J. G. Hudson, X. Da, *J. Geophys. Res.* **101** (D2), 4435 (1996).
14. J. W. Fitzgerald, W. A. Hoppel, M. A. Vietti, *J. Atmos. Sci.* **39**, 1838 (1982).
15. G. P. Frank, U. Dusek, M. O. Andreae, *Atmos. Chem. Phys. Discuss.* **6**, 2151 (2006).
16. Materials and methods are available as supporting material on *Science* Online.
17. M. Shulmann, M. C. Jacobson, R. J. Charlson, R. E. Synovec, T. E. Young, *Geophys. Res. Lett.* **23**, 277 (1996).
18. M. C. Facchini, M. Mircea, S. Fuzzi, R. J. Charlson, *Nature* **401**, 257 (1999).
19. U. Dusek *et al.*, *Geophys. Res. Lett.* **32**, L11802 (2005).
20. J. T. Jayne *et al.*, *Aerosol Sci. Technol.* **33**, 49 (2000).
21. J. P. Putaud *et al.*, *Atmos. Environ.* **38**, 2579 (2004).
22. M. Kanakidou *et al.*, *Atmos. Chem. Phys.* **5**, 1053 (2005).
23. G. P. Frank, U. Dusek, M. O. Andreae, *Atmos. Phys. Chem. Discuss.*, in press.
24. G. Feingold, *Geophys. Res. Lett.* **30**, 1997 (2003).
25. U. Lohmann, K. Broekhuizen, R. Leaitch, N. Schantz, *Geophys. Res. Lett.* **31**, L05108 (2004).
26. B. Ervens, G. Feingold, S. M. Kreidenweis, *J. Geophys. Res.* **110**, D18211 (2005).
27. D. S. Covert, V. N. Kapustin, T. S. Bates, P. K. Quinn, *J. Geophys. Res.* **101**, 6919 (1996).
28. U. Dusek, G. P. Reischl, R. Hitzenberger, *Environ. Sci. Technol.* **40**, 1223 (2006).
29. Z. Levin, A. Teller, E. Ganor, Y. Yin, *J. Geophys. Res.* **110**, D20202 (2005).
30. E. Swietlicki, personal communication.
31. We thank H. Bingemer from the University of Frankfurt and the Taunus Observatory team for their help, B. Fay from the German Weather Service for providing trajectory analysis data, and H. Wernli for help with the trajectory interpretation. The Max Planck Society and the University of Mainz are acknowledged for funding the FACE-2004 measurement campaign. We thank the University of Frankfurt for access to the facilities at the Taunus Observatory for the duration of the FACE-2004 campaign. We thank D. Rosenfeld and Z. Levin for valuable comments on the manuscript.

A New Genus of African Monkey, *Rungwecebus*: Morphology, Ecology, and Molecular Phylogenetics

Tim R. B. Davenport,[1]* William T. Stanley,[2] Eric J. Sargis,[3] Daniela W. De Luca,[1] Noah E. Mpunga,[1] Sophy J. Machaga,[1] Link E. Olson[4]

A new species of African monkey, *Lophocebus kipunji*, was described in 2005 based on observations from two sites in Tanzania. We have since obtained a specimen killed by a farmer on Mount Rungwe, the type locality. Detailed molecular phylogenetic analyses of this specimen demonstrate that the genus *Lophocebus* is diphyletic. We provide a description of a new genus of African monkey and of the only preserved specimen of this primate. We also present information on the animal's ecology and conservation.

A previously unknown monkey from southern Tanzania was recently discovered and described as the new species *Lophocebus kipunji*, depicting the holotype and paratype with photographs (*1*). On 3 August 2005, a subadult male monkey matching the species description of *L. kipunji* (*1*) was found dead in a trap set by a resident farmer in a maize field adjacent to the forest on Mount Rungwe in southwestern Tanzania. The specimen was preserved and deposited at the Field Museum of Natural History (FMNH) in Chicago, USA, as a study skin, skull, and partial skeleton (bones from the right fore- and hindlimbs). Muscle tissue was collected for molecular analyses, and the remaining cadaver was preserved in fluid. Although a subadult, the specimen exhibits features differentiating it from any other known primate species (*1*).

The specimen matches the original description of *L. kipunji* (*1*) in having black eyelids that do not contrast with the color of the face (fig. S1), a crown with a broad erect crest of hair (figs. S1 and S2), long cheek whiskers (fig. S2), and an off-white distal half of the tail [fig. S2 and supporting online material (SOM) text].

The individual was a subadult on the basis of the presence of deciduous canines and premolars, eruption of only the first molars (SOM text), and the lack of a fused suture between the basioccipital and basisphenoid bones (Fig. 1). Although not fully grown, the skull does exhibit some of the features characteristic of *Lophocebus* compared with *Cercocebus* (*2*), such as a relatively narrow zygomatic breadth, zygoma that turn smoothly toward the skull at their posterior ends, and upper and lower margins of the mandible divergent anteriorly (Fig. 1). In the postcranium, the long-bone epiphyses are fused to the diaphyses, but many features are not yet fully developed, including those distinguishing the *Lophocebus*-*Theropithecus*-*Papio* clade from the *Cercocebus*-*Mandrillus* clade (*3*). One postcranial feature, the ratio of scapular width to length, appears to distinguish *L. kipunji* from *Papio*, which has a relatively long and narrow scapula (*3*).

Mangabeys were once considered to be monophyletic based on their phenotypic similarities (*4*), and all species were included in *Cercocebus*. After immunological studies (*5*) and because of cranial differences and a resemblance between *Lophocebus* and *Papio* in some of those features, they were divided into *Cercocebus* and *Lophocebus* (*2*). Characters that have historically been used to unite mangabeys were discounted as being erroneous observations or convergent similarities (*2*). It was stated that *Lophocebus*, unlike *Cercocebus*, has dark eyelids that are not lighter than the facial skin, and the deep suborbital fossae of mangabeys may have evolved independently in relation to facial shortening (*2*). This generic

[1]Wildlife Conservation Society, Southern Highlands Conservation Programme, Post Office Box 1475, Mbeya, Tanzania. [2]Department of Zoology, Field Museum of Natural History, 1400 South Lake Shore Drive, Chicago, IL 60605, USA. [3]Department of Anthropology, Yale University, Post Office Box 208277, New Haven, CT 06520, USA. [4]University of Alaska Museum, 907 Yukon Drive, Fairbanks, AK 99775, USA.

*To whom correspondence should be addressed. E-mail: tdavenport@wcs.org